Implementing an Efficient Feature Pyramid Network with YoloV9 for Lung Nodules Detection using Low-Dose Computed Tomography Images

Sure Sindhurekha
Dept. of ECE
SR University
Warangal, Telangana, India
sindhusure.sure@gmail.com

Sreedhar Kollem
Dept. of ECE
SR University
Warangal, Telangana, India
ksreedhar829@gmail.com

Arun Sekar Rajasekaran
Dept. of ECE
SR University
Warangal, Telangana, India
rarunsekar007@gmail.com

***Abstract*-Early diagnosis of lung cancer is possible by the detection of lung nodules. In order to find such lesions, Computed Tomography (CT) scan images are analyzed by the skilled radiologists, slice by slice. CT scans with lower dosage and resolution are used for preliminary screening. As the lung nodules are small, the effort required by radiologists to process each image is high as it takes a lot of time and the probability of false detection is high. Existing Computer-Aided Detection (CAD) modules like conversion of CT, segmentation of lung nodules, and extraction of features are typically complicated and time-consuming. Thus, a comprehensive image processing system to detect lung nodules is required. In order to eliminate various shortcomings in the classical frameworks, a new deep learning-based lung nodule detection model is suggested in this work. At first, essential Low-Dose CT (LDCT) images for the validation purposes are taken from the benchmark resources. Next, the collected LDCT images are given as input to the lung nodule detection phase. Here, a Fused Network (FusNet) is employed to execute the lung nodules detection process. The FNet is developed by incorporating Feature Pyramid Network (FPN) with You Only Look Once (YoloV9) with Normalized Hybrid Error Loss (NHEL). Finally, the lung nodules detection outcomes are obtained from the FusNet. At last, the efficiency of the developed framework is analyzed over prior techniques by considering various performance measures.**

Keywords-Lung Nodules Detection; Fused Network; Low-Dose Computed Tomography; Lung Cancer; Feature Pyramid Network; You Only Look Once v9

I. INTRODUCTION

Lung cancer is caused by factors such as physical inactivity, poor dietary habits and tobacco use. Among all cancer types, lung cancer results in the highest number of deaths due to smoking issues [6]. After tumors are identified in the lungs, a procedure called excision is performed to evaluate their progression. In order to improve survival rates, detecting and diagnosing malignant nodules at an early stage is necessary [7]. Pulmonary nodules vary in size and location. Moreover, these nodules appear as small, round or oval-shaped regions. Benign nodules are generally smooth and may contain calcifications [8]. Features such as irregular and lobulated borders indicate malignancy. The formation of these nodules is contributed by the lung inflammation [9]. Lung nodules are important imaging markers as it play a vital role in the early screening and diagnosis of lung cancer. Nodules with a diameter of 3 cm or less are classified as pulmonary nodules [10]. These types of nodules are considered as non-cancerous. Detecting malignant nodules contributes to a better prognosis and it enables the application of less invasive treatment methods like radiotherapy and chemotherapy [11].

Lung nodule detection has been carried out using several medical imaging techniques like CT, chest X-rays and Magnetic Resonance Imaging (MRI). CT is widely regarded as the premier method for locating lung nodules. However, it has limitations of false-positive results and exposure to hazardous X-ray radiation [12]. Therefore, researchers have proposed LDCT for lung cancer screening, and it has been shown to reduce lung cancer mortality more effectively than standard X-ray imaging by early detection [13]. Modern deep learning architectures such as MixNet, DenseNet and ResNet have high feature representational efficiency and improved gradient flow that enable more stable and accurate detection of small nodules. In complex thoracic images, feature discrimination is enhanced by the incorporation of attention mechanisms into various detection methods [14]. Conventional approaches still face challenges in detecting nodules smaller than 6 mm, where noise issues and subtle intensity gradients result in false-positive detections. Overfitting is a common issue in traditional transfer learning models and it is caused by data scarcity [15]. Therefore, accurate analysis of complex patterns in lung images is vital for improving lung nodule detection performance. In this work, a lung nodule detection approach using deep learning with an advanced loss function is developed. The following are the contributions.

- To develop a deep learning-assisted network for performing lung nodule detection to ensure accurate identification of nodules from LDCT images. The proposed method is useful in improving the reliability of automated lung cancer screening to support timely diagnosis and minimize mortality risk.
- To design a FusNet model for lung nodule detection by integrating FPN and the YOLOv9 approach along with a new loss function named NHEL. The YOLOv9 model processes the input images and retrieves hierarchical features. These features are processed by FPN model for generating multi-scale feature representations to effectively detect nodules of different sizes. The presence of the YOLOv9 technique ensures fast and efficient lung nodule detection. The class imbalance issue is rectified by the NHEL that helps the FusNet model to improve localization precision.

The organization of the paper is as follows: Sub-division II presents the literature survey of existing studies related to lung

nodule detection. The architectural representation of the proposed lung nodule detection system using LDCT images are provided in Sub-division III. Also, this sub-division describes the dataset collection process. Sub-division IV gives the workflow of the implemented advanced pyramid network along with the proposed loss function for nodule detection. Sub-division V showcases the results obtained from the experiments and Sub-division VI has the conclusion.

II. LITERATURE SURVEY

A. Related Works

In 2024, Harale *et al.* [1] have employed an improved YOLOv5 (iYOLOv5) for lung nodule detection. This model utilized a standard medical imaging dataset for training. Classification of nodules into different structural categories was achieved through hybrid learning models combining convolutional networks with traditional classifiers. This integrated design enhanced the detection and categorization of nodules that was useful for supporting improved diagnostic analysis.

In 2026, Rehman *et al.* [2] have introduced a three-dimensional attention-driven generative framework for lung nodule assessment. This model incorporated detection and segmentation components to localize nodules effectively, while latent feature representations were used for robust classification. Additional integration of patient-specific indicators enabled more personalized predictions and this model was extended with IoT-based monitoring systems for continuous healthcare support.

In 2025, Rodrigues *et al.* [3] have implemented a prototype learning and capsule network-aided technique for lung nodule characterization. This method emphasized structured feature representation by clustering the visual attributes through a loss function formulation. Thus, this module improved interpretability while maintaining effective prediction of nodule malignancy.

In 2025, Farina *et al.* [4] have suggested a spatio-temporal deep learning approach to analyze sequential CT scans for predicting nodule progression. Spatial features were extracted using convolutional networks, while temporal dependencies were modeled through recurrent units enhanced with attention mechanisms. The study also addressed missing temporal data using specialized augmentation and dropout strategies to reduce bias issues.

In 2024, Wang *et al.* [5] have proposed a generative deep learning approach to predict the future growth patterns of lung nodules from imaging data. The designed model enabled improved early-stage risk assessment without requiring actual longitudinal scans. The outcomes demonstrated the potential of generative methods in supporting proactive clinical decision-making.

B. Problem statement

The survival rate of lung cancer is very low. In order to enhance the survival rates of patients, early detection of lung nodules is essential to analyze the abnormal growth of cells. Traditional models are not efficient in accurately recognizing the lung nodules in LDCT scans due to the different densities and shapes of nodules. Thus, obtaining definitive information from imaging data is complex. Some of the other demerits that motivate the development of the suggested nodule detection model are provided below:

- ❖ Missed detections are caused by the existing models as they are not proficient in precisely identifying tiny or low-contrast lung nodules in LDCT scans.
- ❖ Standard loss functions are not sufficient for handling class imbalance and small object detection in medical imaging that result in poor lung nodule detection accuracy.
- ❖ Techniques like Faster R-CNN require more time to process CT scans and they do not analyze features at different scales that affect the efficiency of detecting nodules with different sizes.

Positive aspects and critical limitations of conventional lung nodule detection techniques are given in Table I.

TABLE I. POSITIVE ASPECTS AND CRITICAL LIMITATIONS OF CONVENTIONAL LUNG NODULE DETECTION TECHNIQUES

Author [citation]	Methodology	Features	Challenges
Harale *et al.* [1]	iYOLOv5	• It shows better convergence and enhances the efficiency of the training process that results in lower loss values. • It improves diagnostic accuracy by effective classification of lung nodules.	• This model incurs higher computational demands.
Rehman *et al.* [2]	3D-ConVAT	• It is capable of performing accurate volumetric nodule localization with variational encoding and attention-driven contextual reasoning.	• Data privacy and security issues arise due to the reliance on continuous physiological monitoring through IoT. • The model's performance may be affected by anatomical variability that reduces the generalization efficiency.
Rodrigues *et al.* [3]	Efficient-Proto-Caps	• The use of a loss function aids in clustering lung nodule visual attributes for increasing the interpretability.	• The risk of performance degradation is high.
Farina *et al.* [4]	Spatio-temporal deep learning	• This model integrates spatial features and temporal information for learning the nodule's characteristics accurately. • It prioritizes informative time points to focus on relevant information for malignancy prediction.	• Variations in CT reconstruction filters affect the detection and assessment of nodules. • Robustness of the model against overfitting is low.
Wang *et al.* [5]	GP-WGAN	• It has the potential to improve early diagnosis of lung cancer by predicting future growth patterns of lung nodules. • It enhances risk stratification for an indeterminate nodule.	• It is not suitable for adequately capturing the complex growth patterns of nodules over time.

III. Architectural Representation of Proposed Lung Nodule Detection from Low-Dose Computed Tomography Images

A. Developed Lung Nodule Detection Model

The lung cancer patients' chance of survival is improved by the early and precise identification of lung nodules. However, noise, low contrast and the nodule appearance issues reduce the accuracy of traditional lung nodule detection techniques. In this paper, a deep learning-based lung nodule detection model is suggested to improve detection accuracy and computing efficiency in order to overcome these drawbacks for efficient lung cancer diagnosis. Here, LDCT images are gathered from public repositories as it is useful to ensure standardized validation. LDCT scans are useful for screening purposes due to their lower radiation dose. The gathered images are provided to the developed lung nodule detection system named FusNet. This model combines the advantages of the FPN approach and the YOLOv9 module along with an NHEL function. The proposed model successfully detects lung nodules of different sizes by the combination of FPN with YOLOv9. The FusNet model accurately captures small and big nodules due to the multi-scale feature extraction ability of FPN. Great efficiency in the lung nodule detection process is attained by the employed single-stage detection mechanism YOLOv9. Moreover, this model includes an NHEL function that combines squared and absolute error components to improve the nodule detection accuracy. During training, this hybrid loss function is helpful in improving the convergence, reducing the sensitivity to outliers and increasing the stability of deep learning networks. Thus, the FusNet model provides accurate localization and identification of lung nodules for precise lung cancer screening. The effectiveness of the suggested framework is assessed using different performance indicators in comparison with current approaches. Architectural overview of the proposed lung nodule detection model is visualized in Fig. 1.

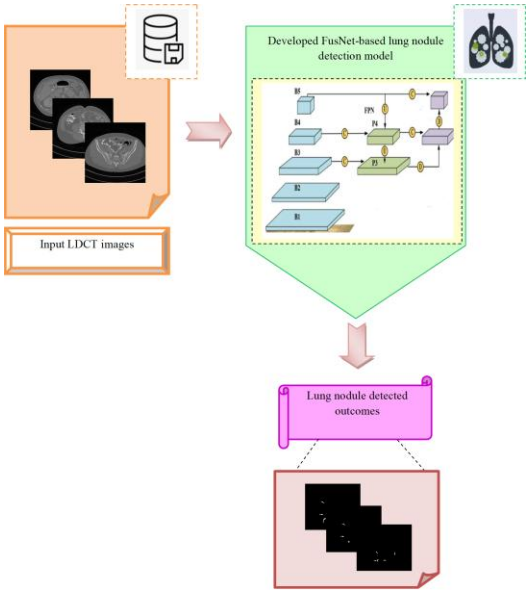

Fig. 1. Architectural overview of the proposed lung nodule detection model

B. Dataset Collection Process

CT Low Dose Reconstruction: This dataset is accessible via the following URL:

https://www.kaggle.com/datasets/andrewmvd/ct-low-dose-reconstruction. LDCT scans are provided in this database, which are helpful for lung nodule detection. Details like slice number as well as the thickness of each image are given. The overall size of this repository is 25.96 GB.

Collected LDCT images are denoted as N_M^{LDCT} . Here, the term M represents the total images.

IV. Workflow Representation of the Implemented Advanced Pyramid Network with Loss Function

A. Yolov9 Model

The lung nodule detection capability is enhanced by the YOLOv9 model [16] as it incorporates multiple structural enhancements. In order to extract features, the backbone of this network adopts RepNCSP-ELAN blocks. This block combines normalized cross-stage partial connections with an efficient large kernel attention mechanism. Due to the integration of large-kernel convolutions with channel-focused attention, the ELAN-based design effectively captures long-range contextual relationships within feature maps.

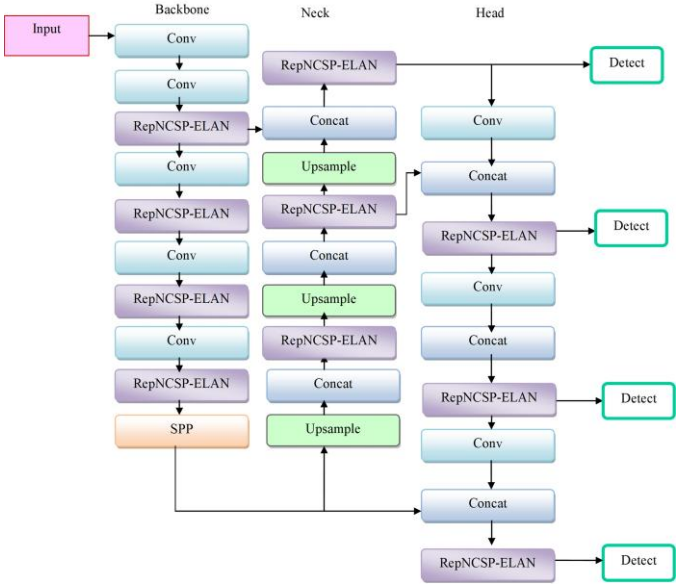

Fig. 2. Structural demonstration of Yolov9

In the YOLOv9 model, RepNBottleneck and RepNCSP components are repeatedly arranged for enabling layered feature representation. In order to refine feature quality, the backbone applies the information bottleneck principle to reduce redundant information and emphasizes the most relevant patterns. In the intermediate stage, the neck utilizes an enhanced path aggregation network to strengthen multi-scale feature fusion for the effective detection of nodules with different sizes. The final stage of the architecture is known as the detection head that assigns class probabilities and compute scores that indicate the object presence within each predicted region. The formulation of the bounding box coordinates in the Yolov9 model is given in Eq. (1).

$$Y_{bx} = -\frac{1}{N}\sum_{a=1}^{N}\sum_{j=1}^{J} g_l \log(\hat{z}_a) \quad (1)$$

In the above expression, the number of bounding box and the samples are represented as J and N, respectively. The predicted probability and ground truth label are indicated as $\hat{z}_a$ and g_l, concurrently. Additionally, asymmetric downsampling modules are incorporated to reduce spatial resolution that is beneficial in preserving important structural details. Structural demonstration of Yolov9 is depicted in Fig. 2.

B. Feature Pyramid Network

The FPN is used to identify tiny-sized lung nodules more effectively [17]. In order to regulate the channel dimensions, each convolutional output is passed through a 1×1 convolution kernel. Then, the upsampling process is performed to integrate high-level feature maps with lower-level features for obtaining features with higher spatial resolution. The FPN is organized into several pyramid levels that operate at different scales. At each level, features are formed by combining outputs from adjacent scales. The construction process starts from the feature map $V5$, which is transformed using a 1×1 convolution to produce a feature scale $F5$. This map is then upsampled and merged with the transformed output of $V4$ to form $F4$. This procedure continues sequentially, then the feature maps $F3$ and $F2$ is generated by combining the upsampled features from the previous level. The mathematical formulation for generating these feature maps is given in Eq. (2)-Eq. (7).

$$F5 = Con_{1\times1}(V5) \quad (2)$$

$$F4 = Us(F5) + Con_{1\times1}(V4) \quad (3)$$

$$F3 = Us(F4) + Con_{1\times1}(V3) \quad (4)$$

$$F2 = Us(F3) + Con_{1\times1}(V2) \quad (5)$$

$$F6 = Con_{3\times3}(F5) \quad (6)$$

$$F7 = Con_{3\times3}(F6) \quad (7)$$

Here, the term Us indicates the upsampling process. To perform downsampling, the feature map $F5$ is processed using a 3×3 convolution to obtain $F6$. Another 3×3 convolution is then applied to $F6$ for attaining $F7$.

C. Developed FusNet for Lung Nodule Detection

The FusNet mechanism is developed by the combination of FPN with the YOLOv9model. FusNet has the advantage of multi-scale feature learning from FPN and the object detection strength of YOLOv9 that is useful for accurate detection of lung nodules from input LDCT images N_M^{LDCT}. The backbone of the Yolov9 network consists of convolutional and RepNCSP-ELAN blocks. Hierarchical feature maps are derived from the input images in the backbone stage. These features are passed to the FPN module, which is presented in the neck region of YOLOv9 to extracts multi-scale feature maps at multiple depths. The higher layers in the FPN learn the deeper semantic information pertinent to lung nodule patterns and the lower layers retain the small spatial details. All feature maps capture complex representations in the LDCT images. In the resultant features, the fine-grained nodule structures are preserved effectively. Each pyramid level in FPN carries identical high-level information with different feature map sizes to preserve semantic consistency across various spatial resolutions. Delicate lung nodule boundaries in LDCT images are maintained without any loss by this network. As the redundancy in feature learning is reduced by the FPN, the computational efficiency is increased. Furthermore, by fusing precise spatial precision with coarse contextual details, the pyramid shape increases localization accuracy by minimizing the influence of surrounding anatomical noise. By enhancing inter-scale communication, the neck stage improves the multi-scale features and it combines the semantic information as well as fine-grained spatial details. Additionally, the neck improves the capacity to localize features for precisely detecting tiny lung nodules. The resultant features are passed to the detection head of the YOLOv9 approach for performing lung nodule detection. The computation for differentiating the background regions and the nodules by YOLOv9 is expressed in Eq. (8).

$$Y_{LN} = -\frac{1}{N}\sum_{a=1}^{N}\left[z_a \log(\hat{z}_a) + (1-z_a)\log(1-\hat{z}_a)\right] \quad (8)$$

Due to the use of FPN-refined features, YOLOv9 gains improved sensitivity to small and low-contrast nodules. Memory efficiency is improved through the use of reversible functions in the YOLOv9 model. The FusNet mechanism is stabilized with the use of NHEL function. The NHEL function is proposed by the combined strengths of squared error and absolute error. The robustness to small variations is improved by the inclusion of absolute error and large errors are minimized by the squared error. The computation of the NHEL function is given in Eq. (9).

$$NHEL = g \times \frac{-2}{100} \times \sum_{a=1}^{g}\left(z_a - \hat{z}_a\right)^2 + \left|z_a - \hat{z}_a\right| \quad (9)$$

Here, the actual and predicted probability is specified by the terms z_a and $\hat{z}_a$, respectively. The total data points are stated as g. The suggested loss function effectively handles slight and significant variations between the actual and predicted nodule regions. The NHEL function stabilizes the training process by maintaining regular gradient updates and reducing sensitivity to outliers. As it offers smoother gradient transitions, NHEL facilitates faster convergence and improves the learning efficiency of the developed FusNet model. Architecture of the developed FusNet-based lung nodule detection is displayed in Fig. 3.

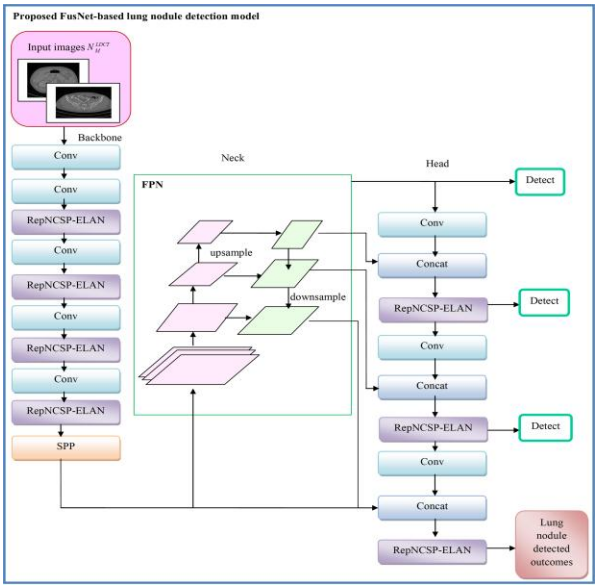

Fig. 3. Architecture of the developed FusNet-based lung nodule detection model

V. Experimental Results

A. Simulation Details

The development of the proposed lung nodule detection model was performed using Python. The effectiveness of the suggested framework was assessed using different performance indicators in comparison with current approaches. Here, techniques like iYoLov5 [1], Efficient-Proto-Caps [3], FPN [17] and Yolov9 [16] were considered for experimental evaluation of the developed technique.

B. Image Results

The lung nodule detected images obtained by the suggested FusNet model is shown in Fig. 4.

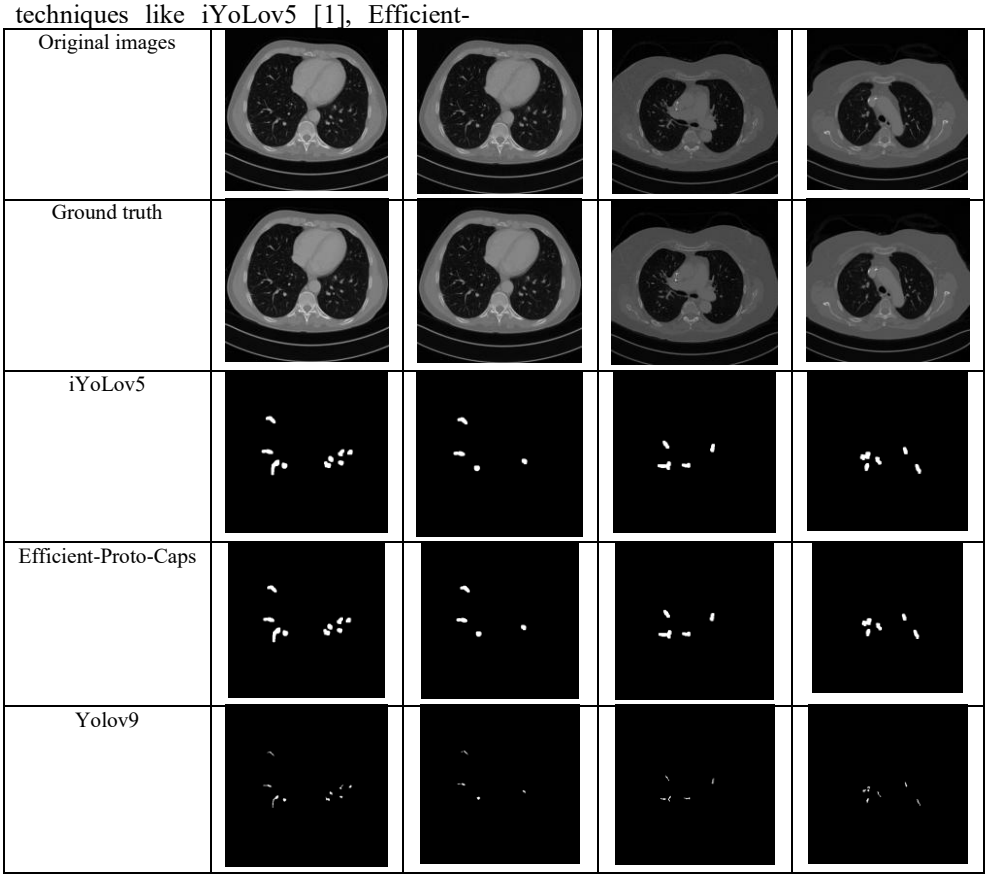

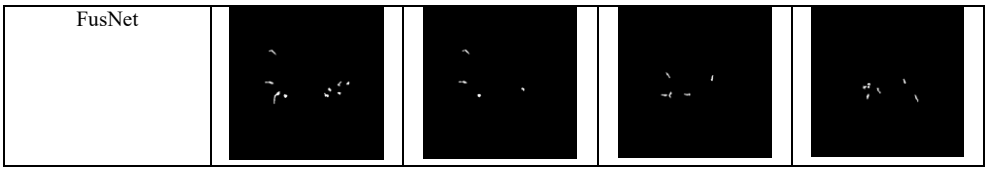

Fig. 4. Lung nodule detected images from the FusNet model

C. Loss Function-based Detection Performance Validation

The lung nodule detection efficiency of the developed FusNet model is verified by comparing its performance with other techniques. The results are taken based on the different loss functions as given in Fig 5. The integration of multi-scale feature extraction through FPN and the efficient single-stage detection capability of YOLOv9 resulted in high F1-score and dice coefficient outcomes in lung nodule detection. The FusNet model achieves an accuracy of over 95% in the detection process when using the novel NHEL function. Due to the limited capability in capturing multi-scale contextual features, the conventional iYOLOv5 model is less efficient in detecting small lung nodules. The slower inference issue due to capsule-based processing in the Efficient-Proto-Caps model, it also resulted in less accuracy. When compared to traditional models such as iYOLOv5, Efficient-Proto-Caps, standard FPN as well as Yolov9 models, the developed FusNet effectively captures fine-grained spatial details and high-level semantic information for detecting small lung nodules in LDCT images.

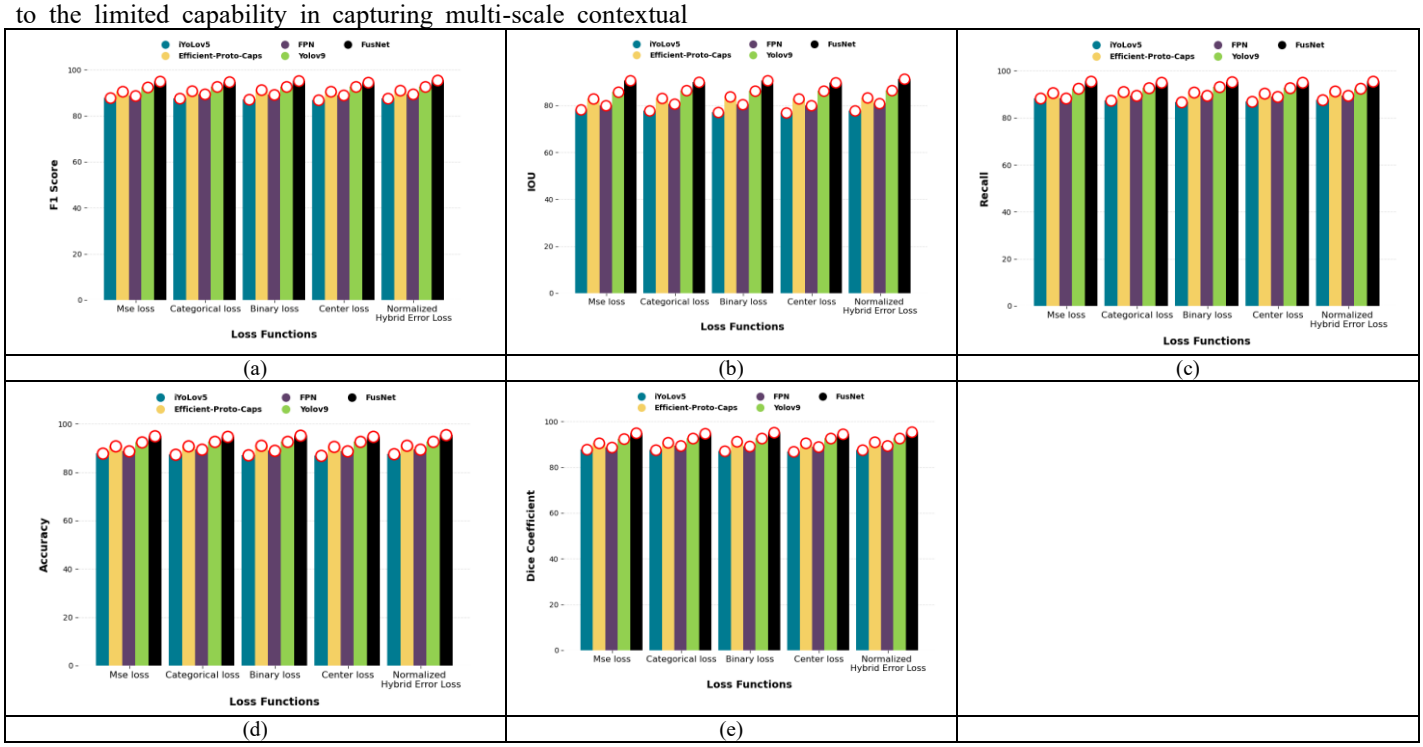

Fig. 5. Loss Function-based Detection Performance Validation of Developed Model with Respect to a) F1 score, b) IOU, c) Recall, d) Accuracy and e) Dice coefficient

D. Effectiveness of the Proposed Model

The effectiveness of the proposed FusNet model is compared with standard Yolov9 approach and the outcomes are exhibited in Fig. 6. The dice coefficient score of the presented FusNet in detecting lung nodule is 95.41%, 94.53%, 95.09%, 95.50% and 95.31% for linear, ReLu, TanH, sigmoid and softmax activation function. As the standard yolov9 module struggles with fine-grained feature representation, it might miss tiny nodules. But, the combination of FPN and NHEL function in the Yolov9 model overcomes the existing issues and results in high accuracy for the lung nodule detection process. Missed detection outcomes are very low when compared to the standard Yolov9 network. At the ReLu activation function, the accuracy of FusNet is 95.51%. FusNet maintains uniform semantic representation across different feature levels that are beneficial for reducing ambiguity between nodules and surrounding regions.

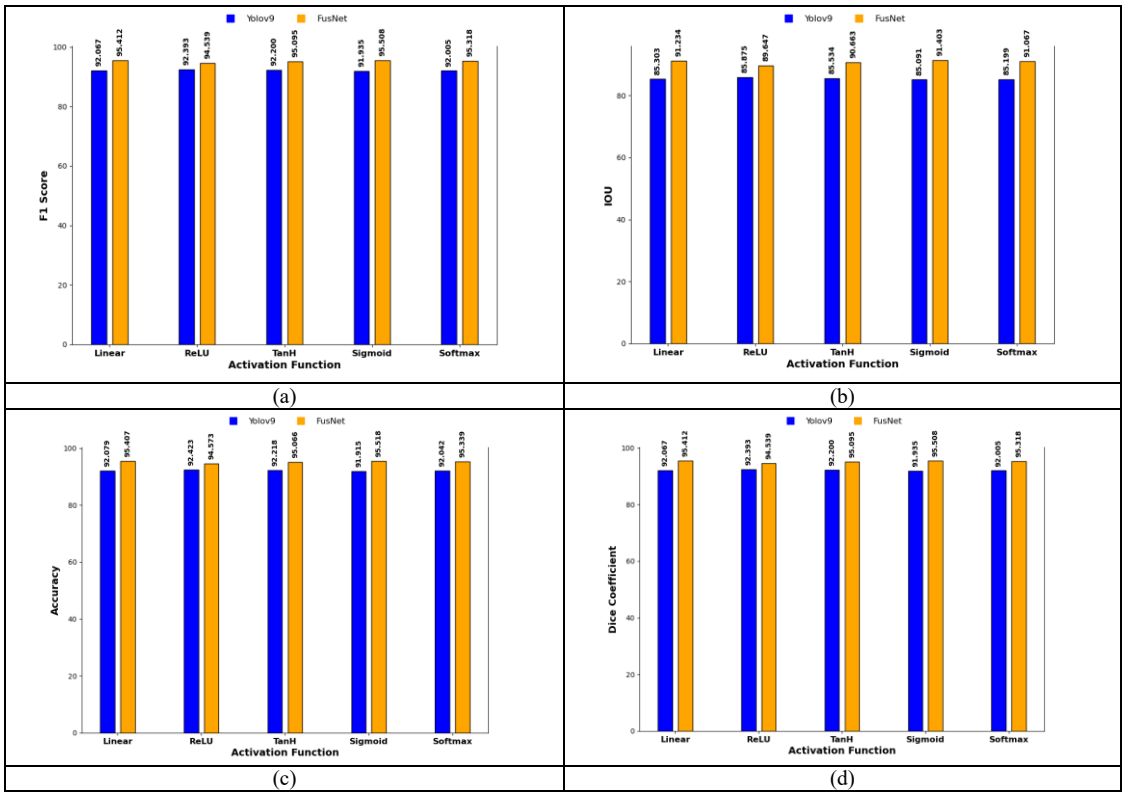

Fig. 6. Effectiveness of the Proposed Model by Means of a) F1 score, b) IOU, c) Accuracy and e) Dice coefficient

E. Computational Efficiency of the Proposed Model

The computational efficiency of the proposed model in detecting lung nodules from LDCT images are analyzed among state-of-the-art models and the final outcomes are given in Table II. At a step per epoch of 100, the accuracy and F1-score of the implemented FusNet model is 94.93% and 94.98%, respectively. The iYolo5 model has a lower detection performance due to its weaker feature representation ability. Moreover, the insufficient multi-scale feature enhancement in the standard Yolov9 model fails to obtain better results in detecting lung nodules. At a step per epoch of 50, the techniques like iYoLov5, Efficient-Proto-Caps, FPN and Yolov9 model obtain a F1-score of 87.40%, 91.22%, 89.11% and 91.92%, but the proposed FusNet mechanism obtained a F1-score of 95.69% in lung nodule detection. The fusion of FPN and Yolov9 helped for efficient extraction of spatial and semantic features that enhanced the detection of small and subtle nodules. Additionally, the inclusion of the NHEL function enhanced the developed FusNet model's resistance to overfitting issues.

TABLE II. COMPUTATIONAL EFFICIENCY OF THE PROPOSED MODEL

Step per epoch	iYoLov5 [1]	Efficient-Proto-Caps [3]	FPN [17]	Yolov9 [16]	FusNet
Accuracy					
50	87.39807	91.18439	88.96271	91.74225	95.6192
100	87.3468	90.8194	89.24225	92.0694	94.93713
150	87.29218	90.94055	88.89984	92.21466	94.54407
200	87.36633	90.54718	89.07166	92.22565	95.05615
250	86.83411	90.90271	89.20807	92.45148	94.84833
F1-score					
50	87.40767	91.22597	89.1155	91.92301	95.69368
100	87.30424	90.80142	89.23999	92.06453	94.98668
150	87.24355	90.89755	88.87448	92.2036	94.53262
200	87.35722	90.58256	89.14988	92.26289	95.06971
250	86.84633	90.903	89.19562	92.44562	94.84643

VI. CONCLUSION

A deep learning-based lung nodule detection model was proposed to improve detection accuracy and computational efficiency for effective lung cancer diagnosis. In this work, LDCT images were collected from public repositories to ensure standardized validation as LDCT scans are widely used for lung cancer screening due to their lower radiation exposure. The collected images were fed into the developed FusNet model for lung nodule detection. The FusNet architecture integrated an FPN with a YOLOv9 detection module along with an NHEL function. The model processed

multi-scale feature representations generated by FPN and used YOLOv9 to perform single-stage detection for identifying lung nodules of varying sizes. The NHEL function was employed during training to support stable convergence. Finally, the efficiency of the developed technique in identifying lung nodules was evaluated using multiple performance metrics in comparison with existing approaches. The accuracy of the FusNet approach in lung nodule detection is 95.61%. Therefore, the developed technique preserved fine-grained nodule structures effectively for accurate nodule detection. In future, data augmentation techniques will be applied to improve robustness against noise and imaging variations. The performance of the detection model will be enhanced by integrating attention mechanisms to focus on more subtle lung nodules.

REFERENCES

[1] A. M. Harale, V. K. Bairagi, E. Boonchieng and M. R. Bachute, "Nodules Detection in Lungs CT Images Using Improved YOLOV5 and Classification of Types of Nodules by CNN-SVM," IEEE Access, vol. 12, pp. 140456-140471, 2024.

[2] Z. U. Rehman, J. Zhao, M. Zaman, Q. Yan, A. Li and A. Akhunzada, "Integrative Deep Diagnostic Architecture: A Convolutional Variational Attention Transformer for Personalized and Multi-Strategy Lung Nodule Detection," IEEE Access, vol. 14, pp. 52054-52066, 2026.

[3] E. M. Rodrigues, M. Gouveia, H. P. Oliveira and T. Pereira, "Efficient-Proto-Caps: A Parameter-Efficient and Interpretable Capsule Network for Lung Nodule Characterization," IEEE Access, vol. 13, pp. 56616-56630, 2025.

[4] Farina, B., R. Carbajo Benito, D. Montalvo-García, D. Bermejo-Peláez, L. Seijo Maceiras, and M. J. Ledesma-Carbayo, "Spatio-temporal deep learning with temporal attention for indeterminate lung nodule classification," Computers in Biology and Medicine, vol. 196, pp. 110813, 2025.

[5] Wang, Yifan, Chuan Zhou, Lei Ying, Heang-Ping Chan, Elizabeth Lee, Aamer Chughtai, Lubomir M. Hadjiiski, and Ella A. Kazerooni, "Enhancing early lung cancer diagnosis: Predicting lung nodule progression in follow-up low-dose CT scan with deep generative model," Cancers, vol. 16, no. 12, pp. 2229, 2024.

[6] Chen, Weitao, Yuntian Zhao, Lu Gao, ZhaoLi Yao, Shenglan Qin, Liangquan Jia, Chong Yao, and Feng Hua, "Construction of a multi-scale feature fusion algorithm for precise lung nodule segmentation," Biomedical Signal Processing and Control, vol. 116, pp. 109568, 2026.

[7] Aro, Renzo Phellan, Stephen Lam, Matthew T. Warkentin, Geoffrey Liu, Brenda Diergaarde, David O. Wilson, Jian-Min Yuan et al., "Integrating deep learning of low-dose computed tomography with clinical data for lung cancer risk prediction," Chest, 2026.

[8] Wang, Jinhua, Zhenchen Zhu, Zhengsong Pan, Weixiong Tan, Wei Han, Zhen Zhou, Ge Hu et al., "Deep learning reconstruction improves computer-aided pulmonary nodule detection and measurement accuracy for ultra-low-dose chest CT," BMC Medical Imaging, vol. 25, no. 1, pp. 200, 2025.

[9] Thakral, Gagan, Umesh Kumar, and Sapna Gambhir, "Hybrid CNN-transformer model with BM3D and YOLOv8 for early detection of lung cancer in low-dose CT scans," Scientific Reports, 2026.

[10] Shaikh, Nishat, Parth Shah, and Bimal Patel, "A meta-heuristic optimization aided automatic technique for lung nodule segmentation and classification using adaptive deep learning mechanism," Biomedical Signal Processing and Control, vol. 120, pp. 110224, 2026.

[11] Li, Runhan, and Barmak Honarvar Shakibaei Asli, "Multi-Task Deep Learning for Lung Nodule Detection and Segmentation in CT Scans," Electronics, vol. 15, no. 4, pp. 736, 2026.

[12] Bocquet, Wesley, Roger Bouzerar, Géraldine François, Antoine Leleu, and Cédric Renard, "Detection of pulmonary nodules on ultra-low dose chest computed tomography with deep-learning image reconstruction algorithm," Journal of Thoracic Imaging, vol. 40, no. 3, pp. e0806, 2025.

[13] Yoo, Seung-Jin, Young Sik Park, Hyewon Choi, Da Som Kim, Jin Mo Goo, and Soon Ho Yoon, "Prospective evaluation of deep learning image reconstruction for Lung-RADS and automatic nodule volumetry on ultralow-dose chest CT," PLOS ONE, vol. 19, no. 2, pp. e0297390, 2024.

[14] Zheng, Zhijuan, Yuying Liang, Zhehao Wu, Qijia Han, Zhu Ai, Kun Ma, and Zhiming Xiang, "Effect of Deep Learning Image Reconstruction Algorithms on Radiomic Features of Pulmonary Nodules in Ultra-Low-Dose CT," Journal of Computer Assisted Tomography, vol. 48, no. 6, pp. 943-950, 2024.

[15] Lan, Huixiang, Xiaobin Liu, Danlin Ou, Sihua Zhong, Hongcheng Zhong, and Mingzhu Liang, "Preoperative localization of pulmonary nodules using ultra-low-dose CT based on artificial intelligence iterative reconstruction," Quantitative Imaging in Medicine and Surgery, vol. 16, no. 3, pp. 236, 2026.

[16] Rajaraman, Sivaramakrishnan, Zhaohui Liang, Zhiyun Xue, and Sameer Antani, "Ensembled YOLO for multiorgan detection in chest x-rays," In Medical Imaging 2025: Computer-Aided Diagnosis, SPIE, vol. 13407, pp. 871-884, 2025.

[17] Tahir, Muhammad Zeeshan, Xingzheng Lyu, Muhammad Nasir, and Sanyuan Zhang, "Advanced image enhancement and a lightweight feature pyramid network for detecting microaneurysms in diabetic retinopathy screening," International Journal of Imaging Systems and Technology, vol. 35, no. 1, pp.e70004, 2025.